

Are cold winters in Europe associated with low solar activity?

This article has been downloaded from IOPscience. Please scroll down to see the full text article.

2010 Environ. Res. Lett. 5 024001

(<http://iopscience.iop.org/1748-9326/5/2/024001>)

View [the table of contents for this issue](#), or go to the [journal homepage](#) for more

Download details:

IP Address: 194.109.159.89

The article was downloaded on 04/04/2012 at 21:14

Please note that [terms and conditions apply](#).

# Are cold winters in Europe associated with low solar activity?

M Lockwood<sup>1,2</sup>, R G Harrison<sup>1</sup>, T Woollings<sup>1</sup> and S K Solanki<sup>3,4</sup>

<sup>1</sup> Space Environment Physics Group, Department of Meteorology, University of Reading, Earley Gate, PO Box 243, Reading RG6 6BB, UK

<sup>2</sup> Space Science and Technology Department, Rutherford Appleton Laboratory, Harwell Campus, Chilton, Didcot, Oxfordshire OX11 0QX, UK

<sup>3</sup> MPI für Sonnensystemforschung, Max-Planck-Straße 2, 37191 Katlenburg-Lindau, Germany

<sup>4</sup> School of Space Research, Kyung Hee University, Yongin, Gyeonggi 446-701, Korea

E-mail: [m.lockwood@reading.ac.uk](mailto:m.lockwood@reading.ac.uk)

Received 12 March 2010

Accepted for publication 31 March 2010

Published 14 April 2010

Online at [stacks.iop.org/ERL/5/024001](http://stacks.iop.org/ERL/5/024001)

## Abstract

Solar activity during the current sunspot minimum has fallen to levels unknown since the start of the 20th century. The Maunder minimum (about 1650–1700) was a prolonged episode of low solar activity which coincided with more severe winters in the United Kingdom and continental Europe. Motivated by recent relatively cold winters in the UK, we investigate the possible connection with solar activity. We identify regionally anomalous cold winters by detrending the Central England temperature (CET) record using reconstructions of the northern hemisphere mean temperature. We show that cold winter excursions from the hemispheric trend occur more commonly in the UK during low solar activity, consistent with the solar influence on the occurrence of persistent blocking events in the eastern Atlantic. We stress that this is a regional and seasonal effect relating to European winters and not a global effect. Average solar activity has declined rapidly since 1985 and cosmogenic isotopes suggest an 8% chance of a return to Maunder minimum conditions within the next 50 years (Lockwood 2010 *Proc. R. Soc. A* **466** 303–29): the results presented here indicate that, despite hemispheric warming, the UK and Europe could experience more cold winters than during recent decades.

**Keywords:** regional climate, solar variability, blocking

## 1. Introduction

Lower winter temperatures were common in Europe during the second half of the 17th century, famously allowing frost fairs to be held on the Thames in London before riverine developments increased the flow rate. These cold winters coincided with the Maunder minimum in solar activity when the Sun remained virtually free of sunspots for almost 50 years [3, 4]. However, establishing that this was not just a chance occurrence requires that the relationship continue to hold over a long interval, such that cold European winters become less frequent when solar activity is high and then more common again when solar activity falls. Various indicators show that during the recent minimum of the 11 year sunspot cycle, the Sun has been quieter

than at any time in the previous 90 years [1, 2]. This yields an opportunity for a better test of the relationship between solar activity and cold European winters. To do this, we require two long and homogeneous time series: one which quantifies solar outputs relevant to seasonal/regional climate and the other relevant to European winter temperatures. We here use the Central England temperature (CET) data set which is the world's longest instrumental record of temperature and extends back to 1659, at the start of the Maunder minimum [5, 6]. The CET covers a spatial scale of order 300 km which makes it a 'small regional' climate indicator [8], and to an extent it will reflect changes on both regional European (~3000 km) and hemispheric scales [8]. In winter, the North Atlantic Oscillation (NAO), and associated changes in thermal

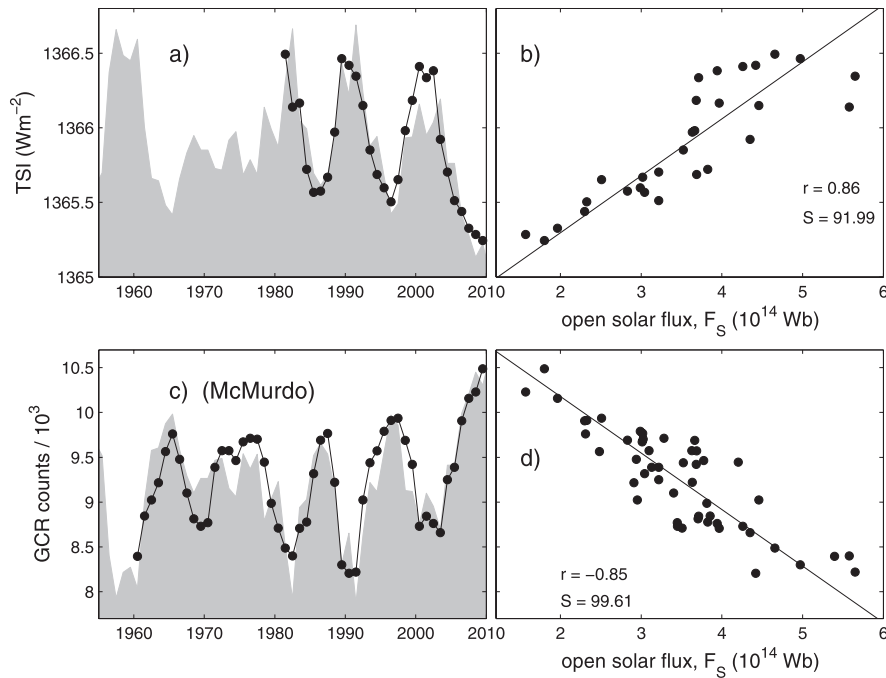


**Figure 1.** The relationship of open solar flux,  $F_S$ , derived from geomagnetic observations [1, 8], with (top) the total solar irradiance, TSI, and (bottom) galactic cosmic ray fluxes (GCRs). We use the PMOD TSI data composite [12], because it agrees best with modelling using solar magnetograph data [13, 2]. GCRs are here quantified by the count rate recorded by the Antarctic McMurdo neutron monitor. (a) and (c) show temporal variations in which the grey areas are the  $F_S$  variation, scaled using the linear regression fits that are shown in the corresponding scatter plots in (b) and (d). Correlation coefficients  $r$  and their statistical significance levels  $S$  (in %) are given. Optimum lags are used (defined as positive for lagged  $F_S$ ), which are zero for the cosmic ray data and  $-1$  year for TSI.

advection, contribute a large fraction of the observed variability of CET [8]. The observed increasing trend in the NAO between 1965 and 1995 may have contributed considerably to the warming trend in European regional temperatures (including CET) in winter [9] and solar modulation of the NAO has been suggested as a cause of the cold European winters experienced during the Maunder minimum [3]. Recent studies of solar influence on the phenomenon of jet stream ‘blocking’ [7] are consistent with these ideas.

## 2. Centennial solar variability

To quantify solar activity, we use annual means of the open solar magnetic flux [10],  $F_S$ , derived from geomagnetic activity indices (with allowance for effects of structure in the solar wind [1]). This derivation of  $F_S$  makes use of the fact that different measures of the fluctuation level in Earth’s magnetic field correlate strongly, but with differences that are statistically significant, with different combinations of solar wind parameters: this means that they can be used in combination to reconstruct past variations, including that in  $F_S$ , the total magnetic flux dragged out of the Sun by the solar wind flow. Comparison with satellite observations shows that the method is extremely reliable (see figure 2(c)), even during the current exceptional solar minimum.

Figure 1 shows that  $F_S$  is highly anticorrelated with cosmic ray fluxes and also correlates very well (with a lag of 1 year) with total solar irradiance (TSI). These correlations are at the centre of a relationship between TSI and solar-modulated

cosmogenic isotopes, which is conventionally assumed in palaeoclimate studies [11]. As well as yielding both the lowest  $F_S$  and TSI seen during the space age, the current solar minimum has seen an unprecedented maximum in cosmic rays detected by high-latitude neutron monitors [2]. Hence recent data are showing that the correlations apparent in 11 year solar cycle variations also apply, at least in part, to longer-term drifts in solar activity [2, 12, 13]. The black line in figure 2(c) shows that  $F_S$  from geomagnetic activity compares well with *in situ* interplanetary measurements (black dots) [1]. This sequence has been extended back to the Maunder minimum (mauve line) using the model of Vieira and Solanki [14] based on the observed sunspot number  $R$ , and in very good agreement with both cosmogenic isotope data and reconstructions of TSI [15, 16]. Note that this model for  $F_S$  allows for two time constants for the loss of open solar flux following its emergence. The longer of these two time constants is a few years which means that after a prolonged period of very low emergence of new open flux (associated with very low  $R$ ), for example during the Maunder minimum,  $F_S$  falls to considerably lower values than during even the Dalton minimum (around 1815), when the minimum in  $R$  was not so deep and was shorter lived. A key point is that  $F_S$  shows centennial-scale variations as well as the 11 year solar cycle, such that both solar maxima and minima exhibit long-term change. This contrasts with  $R$  which shows long-term changes in its solar maximum peaks but almost no drift in solar minimum values. In this respect, both cosmogenic isotopes and reconstructions of TSI resemble  $F_S$  and not  $R$ . In other

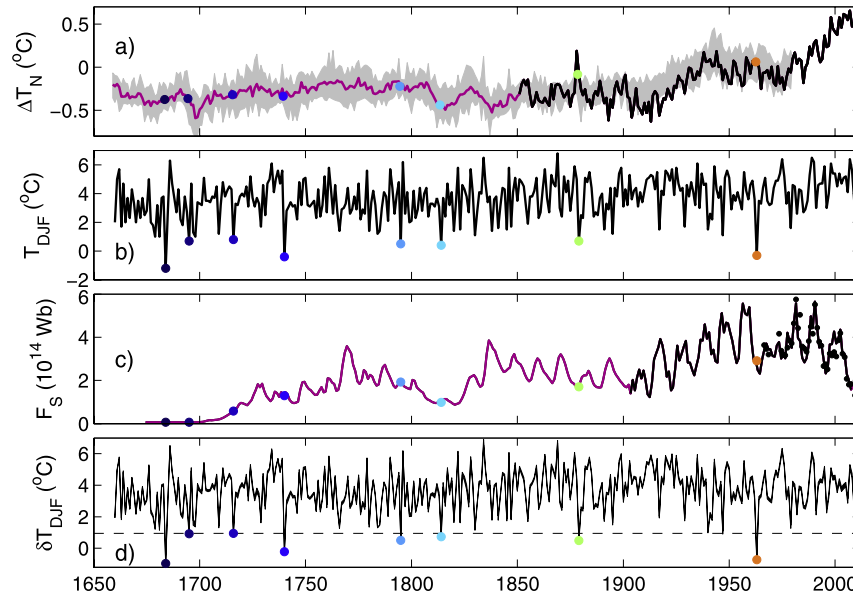


**Figure 2.** Variations since the mid-17th century of the following. (a) The mean northern hemisphere temperature anomaly,  $\Delta T_N$ : black shows the HadCRUT3v compilation of observations [17], mauve shows the median of an ensemble of 11 reconstructions (individually intercalibrated with the HadCRUT3v NH data over the interval 1850–1950) based on tree ring and other proxy data [18–23]. The decile range is given by the area shaded grey (between upper and lower decile values of  $\Delta T_U$  and  $\Delta T_L$ ). (b) Average winter Central England Temperatures (CET) [5, 6] for December, January and February,  $T_{DJF}$ . (c) The open solar flux,  $F_S$ , corrected for longitudinal solar wind structure: dots are annual means of interplanetary satellite data; the black line after 1905 is derived from ground-based geomagnetic data [1]; and the mauve line is a model based on observed sunspot numbers [14]. Both curves show 1 year means. (d) Detrended winter CET,  $\delta T_{DJF}$ , obtained by subtracting the best-fit variation of  $\Delta T_N$ , derived using the regressions shown in figure 3(b): the width of the line shows the difference resulting from the use of  $\Delta T_N = \Delta T_U$  and  $\Delta T_N = \Delta T_L$  prior to 1850. In all panels, dots are for years with  $\delta T_{DJF} < 1^\circ\text{C}$  (the dashed horizontal line in (d)), colour-coded by year using the scale in figure 3(a). Data for the winter 2009/10 are provisional.

words, whereas sunspot numbers give the impression that the Sun returns to almost the same base-level state at each sunspot minimum,  $F_S$ , TSI reconstructions and cosmogenic isotopes all show that this is not the case.

### 3. Winter temperatures in Central England

Figure 2(b) shows the seasonal December/January/February (DJF) means,  $T_{DJF}$ , of the CET record which is representative of a roughly triangular area between Lancaster, London and Bristol. The data after 1974 have been adjusted to allow for urban warming, achieved by comparing the modern data from long-established stations with the available (shorter) data sequences from stations in rural areas [6]. To identify regional effects, we compare with average temperature anomalies for the whole of the northern hemisphere. We use annual means (centred on 1 January) of the HadCRUT3v compilation of northern hemisphere (NH) observations [17], which is available for 1850 onwards (shown in black in figure 1(a)), and extend these data back to 1659 using an ensemble of 11 reconstructions based on a wide variety of proxies. The reconstructions used are: d’Arrigo *et al* ‘STD’ and ‘RCS’ [18]; Mann *et al* ‘EIV’ and ‘CPS’ [19]; Smith *et al* [20]; Ammann and Wahl [21]; Jones and Mann [22]; and the reconstructions calibrated by Briffa *et al* [23]. The results presented here use the median of this ensemble for each year (the mauve line in figure 1(a)) and the decile range (between  $\Delta T_U$  and  $\Delta T_L$ ) shaded in grey. We use the upper decile  $\Delta T_U$  (the second

highest of the 11 reconstructions) and the lower decile  $\Delta T_L$  (the second lowest) to test the dependence of our results on the reconstruction for before 1850. The change in average hemispheric temperature between pre-industrial times (taken here to be 1650–1750) and the past decade is  $0.69^\circ\text{C}$ ,  $0.86^\circ\text{C}$  and  $1.03^\circ\text{C}$  using, respectively,  $\Delta T_U$ , the median  $\Delta T_N$  and  $\Delta T_L$ .

Figure 3(a) shows a scatter plot of  $T_{DJF}$  against  $F_S$ , with the points colour-coded by year. More recent years (red points) are associated with higher  $F_S$  and  $T_{DJF}$ , but the linear correlation is low ( $r = 0.23$ ) and the dark blue points show that a very wide range of  $T_{DJF}$  occurred even during the Maunder minimum. However, figure 3(b) reveals that the scatter of  $T_{DJF}$  against  $\Delta T_N$  (using the median values before 1850) is almost as large ( $r = 0.25$ ). This stresses the great variability of a regional and seasonal temperature (here the winter CET data) around the hemispheric mean. We investigate the variability about the trend by detrending the DJF CET data using the linear ordinary least squares regression fits (of slope  $s$ ) shown in 3(b). Hence our findings relate solely to a winter regional temperature variation about the global trends (the attribution of causes of the latter having been extensively discussed elsewhere (e.g., [24])). The regressions were also carried out using  $\Delta T_U$  and  $\Delta T_L$  before 1850 and the grey area in figure 3(b) is bounded by these two fits. The data are detrended to give  $\delta T_{DJF} = T_{DJF} - s\Delta T_N$  (see figure 2(d): in this plot the width of the line gives the difference between using  $\Delta T_U$  and  $\Delta T_L$  for  $\Delta T_N$  prior to 1850). We investigate the effect of the detrending by repeating our analysis for  $s = 1$  and 0.

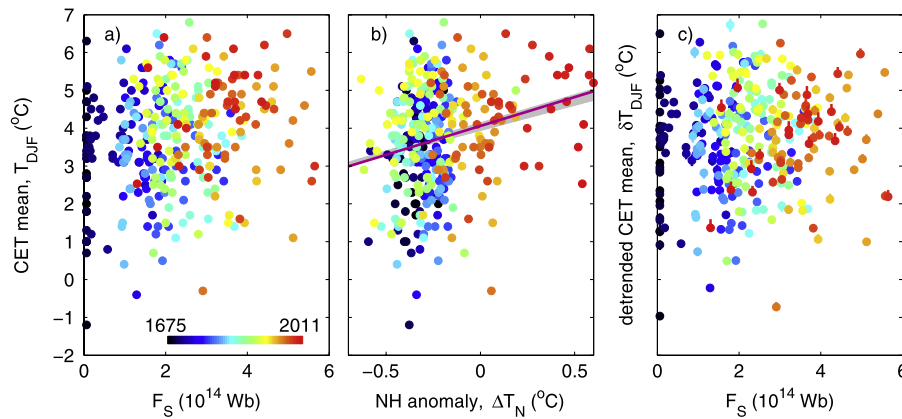


**Figure 3.** Scatter plots of mean winter CET,  $T_{\text{DJF}}$ , as a function of annual means of (a) the open solar flux,  $F_S$  and (b) the mean northern hemisphere temperature anomaly,  $\Delta T_N$ . Points are coloured according to the date using the scale shown in (a). The line in (b) is the ordinary least squares linear regression fit and the grey area is bounded by the corresponding regression fits using  $\Delta T_L$  and  $\Delta T_U$  before 1850. The correlation coefficients for (a) and (b) are 0.23 and 0.25 (significant at the 99.1% and 99.6% levels). (c) Same as (a), but for the detrended winter CET data  $\delta T_{\text{DJF}}$ , as shown in figure 2(d); the vertical bars show the difference caused by using the range of  $\Delta T_N$  between  $\Delta T_L$  and  $\Delta T_U$  before 1850.  $F_S$  values are lagged by  $-1$  year as in the upper panels of figure 1.

#### 4. Solar influence on regional winter anomalies

Figure 3(c) plots  $\delta T_{\text{DJF}}$  against  $F_S$ , with vertical error bars showing the effect of using  $\Delta T_U$  and  $\Delta T_L$  on each point (usually these are smaller than the dots used). Clearly any solar control is subtle and far from being the only factor causing variability: for example, the dark blue dots are all from the Maunder minimum and yet exhibit almost the full range of  $\delta T_{\text{DJF}}$ . However, particularly clear is an absence of points in the low- $\delta T_{\text{DJF}}$ /high- $F_S$  quadrant (bottom right) of the plot, showing that the coldest UK winters tend to have occurred at low solar activity. To investigate this further, we divide the data into two subsets, using a variable threshold value in  $F_S$ , denoted by  $f$ . We consider differences between the distributions of  $\delta T_{\text{DJF}}$  for  $F_S > f$  and  $F_S \leq f$ . Figure 4(b) shows the median values (thick lines surrounded by grey areas) and mean values (thin lines surrounded by yellow areas) of these two subsets as a function of  $f$ : in both cases, the shaded areas show the effect of using  $\Delta T_U$  and  $\Delta T_L$  prior to 1850. Figure 4(c) shows the number of samples in the subsets. Both mean and median  $\delta T_{\text{DJF}}$  for  $F_S > f$  (in red) are greater than for  $F_S \leq f$  for all  $f$ . Figure 4(a) presents the statistical significance of these differences, testing the probability  $p$  of the null hypothesis that solar activity has no effect on  $\delta T_{\text{DJF}}$ , i.e. that the distributions of the two subsets cannot be distinguished. The two dashed lines show the 90% and 95% confidence levels that the distributions differ. The green line gives the results of Student's  $t$  test on the difference in the means. This is a parametric test (it assumes a normal distribution of values), non-robust at small sample numbers. But similar results (mauve line) are obtained from the non-parametric Mann–Whitney  $U$  (Wilcoxon) test of the difference in the medians and of the distribution shapes, which is suitable for small sample numbers. In addition, black dots show where the non-parametric Kolmogorov–Smirnov (KS) test of the cumulative distribution reveals differences significant at the 90% level. The grey area is bound by results obtained from the

$U$  test using  $\Delta T_U$  and  $\Delta T_L$  (which give the upper and lower limits to  $(1 - p)$ , respectively). The vertical cyan lines in figure 4 show the 2009 value of  $F_S$ . Note that low solar activity gives lower mean and median  $\delta T_{\text{DJF}}$  at all  $f$ , but for large  $f$  the statistical significance of the differences is lower. However for most  $f$  below the median  $F_S$ , the difference is significant at about the 95% level for the median reconstructed  $\Delta T_N$  (and generally in the range 85–99% for  $\Delta T_L$  and  $\Delta T_U$ ). Note that figure 4 uses  $s = 1.42 \pm 0.09$  from the linear regressions shown in figure 3(b), and simply adopting the difference between  $T_{\text{DJF}}$  and  $\Delta T_N$  as the indicator of the regional climate anomaly ( $s = 1$ ) would leave a residual warming trend in the CET data which raises the statistical significance to above 99% for almost all  $f$  and for all  $\Delta T_N$  reconstructions. If we restrict our analysis to data before 1900 (when anthropogenic effects on CET are negligible [8]) we obtain almost exactly the same results as are shown in figure 4 without detrending the data ( $s = 0$ ). On the other hand, if we use data for after 1900 with  $s = 0$  we can only reject the null hypothesis at the 10–70% level (depending on  $f$ ) with typical values around only 30%. Thus we see a coherent relationship that has applied at all times from the Maunder minimum to the present day only when we detrend the data to allow for the hemispheric temperature change.

We also carried out an analysis on the  $F_S$  distributions for  $\delta T_{\text{DJF}} \leq \tau$  and  $\delta T_{\text{DJF}} > \tau$  where  $\tau$  is a variable threshold. The coldest eight winters (relative to the northern hemisphere trend), defined by  $\delta T_{\text{DJF}} \leq \tau = 1^\circ\text{C}$ , occurred in 1684, 1695, 1716, 1740, 1795, 1814, 1879 and 1963 (marked with coloured dots in figure 2). The mean and median  $F_S$  for these years is 45% lower than for all other years. Irrespective of the  $\Delta T_N$  proxy reconstruction used, the non-parametric  $U$  and KS tests reject the null hypothesis at  $>99.99\%$  level for this  $\tau$ . The winter of 2009/10 is the 18th coldest, relative to the northern hemisphere trend. (From  $T_{\text{DJF}}$ , 2008/9 and 2009/10 (provisional data) are in the coldest 43% and 17% of the 350 winters studied; however, relative to the trend they

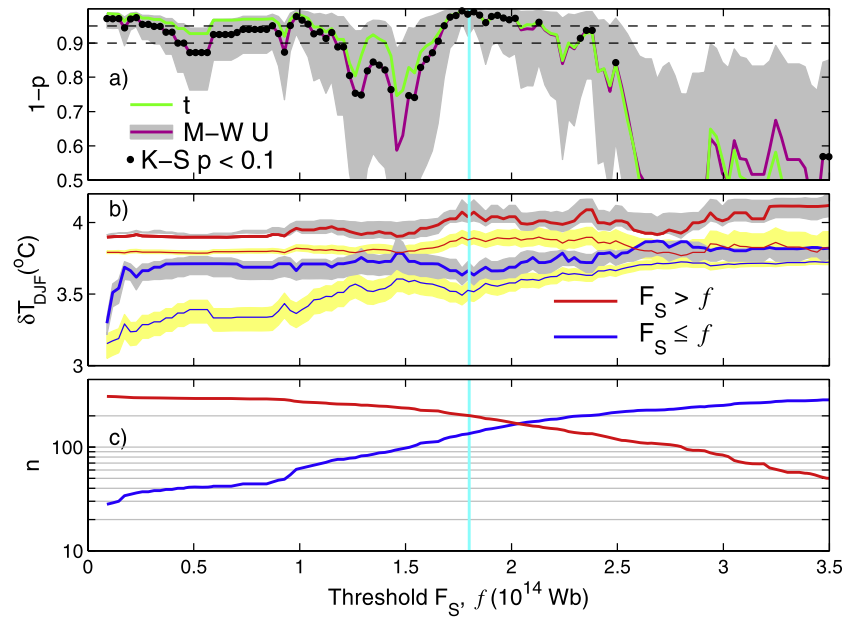


**Figure 4.** Statistical parameters for populations with  $F_S > f$  and  $F_S \leq f$  as a function of the threshold value  $f$ . (a)  $(1 - p)$ , where  $p$  is the  $p$ -value for the null hypothesis that the distribution of  $\delta T_{DJF}$  values is the same for these two independent data subsets. The mauve line and grey area give the significance of the difference of the median values evaluated using the Mann–Whitney  $U$  (Wilcoxon) test: the mauve line is using the median  $\Delta T_N$  before 1850, the upper boundary of the grey area is for  $\Delta T_U$  and the lower boundary is for  $\Delta T_L$ . Where the Kolmogorov–Smirnov test yields differences significant at the  $>90\%$  level is shown by the black dots. The horizontal dashed lines give the 90% and 95% significance levels. The green line is the significance of difference between the mean values, computed using Student’s  $t$  test. (b) The median (thick lines) and mean (thin lines) values for the two subsets (red for  $F_S > f$  and blue for  $F_S \leq f$ ). The grey area shows the range of medians using  $\Delta T_U$  and  $\Delta T_L$  and the underlying yellow area is the corresponding range for the mean values. (c) The number of annual means,  $n$ , in the two subsets. The vertical cyan lines mark the mean  $F_S$  for 2009. Note that this figure employs  $s = 1.42 \pm 0.09$  from figure 3(b) in  $\delta T_{DJF} = T_{DJF} - s \Delta T_N$ : the use of  $s = 1$  results in differences that are significant at the  $>99\%$  at almost all  $f$  and the use of  $s = 0$  gives results very similar indeed to this figure, provided the data are restricted to before 1900.

are in the coldest 15% and 5.3%.) There are 26 UK winters with  $\delta T_{DJF} \leq \tau = 1.8^\circ\text{C}$ , for which the mean and median  $F_S$  are 28% and 23% lower than for all other years. This is significant at the 99% level (96.5% and 99.9% for  $\Delta T_L$  and  $\Delta T_U$  respectively).

## 5. Discussion and implications for the future

The results presented in section 4 allow rejection of the null hypothesis, and hence colder UK winters (relative to the longer-term trend) can therefore be associated with lower open solar flux (and hence with lower solar irradiance and higher cosmic ray flux). A number of mechanisms are possible. For example, enhanced cooling through an increase in maritime clouds may have resulted from the cosmic ray flux increase [25]. Alternatively, tropospheric jet streams have been shown to be sensitive to the solar forcing of stratospheric temperatures [26]. This could occur through disturbances to the stratospheric polar vortex [27] which can propagate downwards to affect the tropospheric jets, or through the effects of tropical stratospheric temperature changes on the refraction of tropospheric eddies [28]. Interestingly, early instrumental records from the end of the 17th century indicate an increased frequency of easterly winds influencing the UK temperatures [29]. This has also been deduced from indirect proxies [30, 31], including the spatial patterns of

changes in recorded harvest dates [32]. This suggests a link with the incidence of long-lived winter blocking events in the eastern Atlantic at low solar activity [33, 34]. These extensive and quasi-stationary anticyclones are characterized by a reversed meridional gradient of geopotential height and easterly winds [7, 33, 35]. Blocking episodes can persist for several weeks, leading to extended cold periods in winter as the mild maritime westerly winds are replaced by continental north-easterlies and the land surface cools under cloudless skies. In particular, long-lived Atlantic blocking events at more eastward locations have been found to be more prevalent at sunspot minimum than at higher solar activity, an asymmetry that is enhanced by the phase of the quasi-biennial oscillation, and this leads to colder winters in Europe [7]. This evidence suggests that changes in the occurrence of blocking could be acting to amplify the solar-induced perturbations to the tropospheric jet stream [26]. Blocking events have been shown to modulate the stratosphere via upward propagating planetary wave disturbances, but the magnitude, extent and lag of the correlations over Europe strongly suggest that the perturbation to the stratospheric wind pattern can, in turn, influence the blocking [35]. This feedback may be the mechanism by which solar-induced changes to the stratosphere influence European blocking events. Other evidence supports this idea. For example, changed position and frequency of blocking events may be seen as a manifestation of modes of low-frequency circulation variability which have been found to respond

to solar activity [36] giving increased/decreased frequencies of easterly/westerly circulation patterns over Europe under conditions of low solar activity [37]. Winter CET values are known to be strongly modulated by the NAO [8] and modelling has shown that stratospheric trends over recent decades, along with downward links to surface, are indeed strong enough to explain much of the prominent trend in the NAO and hence regional winter climate in Europe between the 1960s and the 1990s [9]. It has been reported that geomagnetic activity rather than solar activity has a stronger statistical relationship to the NAO [38] which, given that the former is highly correlated with  $F_S$  (indeed  $F_S$  used here is derived from geomagnetic activity data) is consistent with the effect of  $F_S$  on Central England Temperatures revealed here. Our subsequent studies (not reported here) on solar modulation of various blocking indices have confirmed previous studies [7], and we stress that this phenomenon is largely restricted to Europe and not global in extent [41].

This connection is of particular interest because of recent changes in the Sun. Studies of isotopes generated in the atmosphere by galactic cosmic rays show that the Sun has been exceptionally active during recent decades [39]. This grand solar maximum has persisted for longer than most previous examples in the cosmogenic isotope record and is expected to end soon [40]. The decline in  $F_S$  since about 1985 (see figure 2(c)) is consistent with this prediction [1] and a recent study of the past behaviour of cosmogenic isotopes [2] suggests an  $\sim 8\%$  chance that the Sun could return to Maunder minimum conditions within the next 50 years. The connections reported here indicate that, despite hemispheric warming, Europe could well experience more frequent cold winters than during recent decades.

Lastly, one can invert the title of this paper and ask ‘Does the occurrence of lower/higher solar activity make a cold/warm winter in Europe more likely (than the climatological mean)?’ Our results strongly suggest that it does, which has implications for seasonal predictions.

## Acknowledgments

The CET data are provided by the UK Meteorological Office and the HadCRUT3v data set are compiled by the UK Meteorological Office and the Climate Research Unit, University of East Anglia, UK. The northern hemisphere temperature reconstructions were obtained via the World Data Centre (WDC) for Paleoclimatology, Boulder, USA and the interplanetary and geomagnetic data via the WDC for Solar Terrestrial Physics, Chilton, UK. The cosmic ray data were generated by the Bartol Research Institute, University of Delaware, USA, and the PMOD TSI data composite by the World Radiation Centre, Davos, Switzerland. We thank the many scientists who contributed to these data sets and others for valuable discussions. We also thank Luis Eduardo Vieira of MPI, Lindau, for the open solar flux reconstruction. The work of SK has been partially supported by WCU grant No. R31-10016 funded by the Korean Ministry of Education, Science and Technology.

## References

- [1] Lockwood M, Rouillard A P and Finch I D 2009 The rise and fall of open solar flux during the current grand solar maximum *Astrophys. J.* **700** 937–44
- [2] Lockwood M 2010 Solar change and climate: an update in the light of the current exceptional solar minimum *Proc. R. Soc. A* **466** 303–29
- [3] Shindell D T, Schmidt G A, Mann M E, Rind D and Waple A 2001 Solar forcing of regional climate change during the Maunder minimum *Science* **294** 2149–52
- [4] Mann M E 2002 Little ice age *Encyclopedia of Global Environmental Change* vol 1 *The Earth System: Physical and Chemical Dimensions of Global Environmental Change* ed M C MacCracken and J S Perry (New York: Wiley) pp 504–9 (ISBN 0-471-97796-9)
- [5] Manley G 1974 Central England Temperatures: monthly means 1659 to 1973 *Q. J. R. Meteorol. Soc.* **100** 389–405
- [6] Parker D E, Legg T P and Folland C K 1992 A new daily Central England Temperature Series, 1772–1991 *Int. J. Climatol.* **12** 317–42
- [7] Barriopedro D, García-Herrera R and Huth R 2008 Solar modulation of Northern Hemisphere winter blocking *J. Geophys. Res.* **113** D14118
- [8] Karoly D J and Stott P A 2006 Anthropogenic warming of central England temperature *Atmos. Sci. Lett.* **7** 81–5
- [9] Scaife A A, Knight J R, Vallis G K and Folland C K 2005 A stratospheric influence on the winter NAO and North Atlantic surface climate *Geophys. Res. Lett.* **32** L18715
- [10] Lockwood M, Stamper R and Wild M N 1999 A doubling of the sun’s coronal magnetic field during the last 100 years *Nature* **399** 437–9
- [11] Lockwood M 2006 What do cosmogenic isotopes tell us about past solar forcing of climate? *Space Sci. Rev.* **125** 95–109
- [12] Fröhlich C 2009 Evidence of a long-term trend in total solar irradiance *Astron. Astrophys.* **501** L27–30
- [13] Wenzler T, Solanki S K and Krivova N A 2009 Reconstructed and measured total solar irradiance: is there a secular trend between 1978 and 2003? *Geophys. Res. Lett.* **36** L11102
- [14] Vieira L E A and Solanki S K 2010 Evolution of the solar magnetic flux on time scales of years to millennia *Astron. Astrophys.* **509** A100
- [15] Steinhilber F, Beer J and Fröhlich C 2009 Total solar irradiance during the Holocene *Geophys. Res. Lett.* **36** L19704
- [16] Krivova N A, Balmaceda L and Solanki S K 2007 Reconstruction of solar total irradiance since 1700 from the surface magnetic flux *Astron. Astrophys.* **467** 335–46
- [17] Brohan P, Kennedy J J, Harris I, Tett S F B and Jones P D 2006 Uncertainty estimates in regional and global observed temperature changes: a new dataset from 1850 *J. Geophys. Res.* **111** D12106
- [18] d’Arrigo R, Wilson R and Jacoby G 2006 On the long-term context for late twentieth century warming *J. Geophys. Res.* **111** D03103
- [19] Mann M E, Zhang Z, Hughes M K, Bradley R S, Miller S K, Rutherford S and Ni F 2008 Proxy-based reconstructions of hemispheric and global surface temperature variations over the past two millennia *Proc. Natl Acad. Sci.* **105** 13252–7
- [20] Smith C L, Baker A, Fairchild I J, Frisia S and Borsato A 2006 Reconstructing hemispheric-scale climates from multiple stalagmite records *Int. J. Climatol.* **26** 1417–24
- [21] Ammann C M and Wahl E R 2007 The importance of the geophysical context in statistical evaluations of climate reconstruction procedures *Clim. Change* **85** 71–88
- [22] Jones P D and Mann M E 2004 Climate over past millennia *Rev. Geophys.* **42** RG2002
- [23] Briffa K R, Osborn T J, Schweingruber F H, Harris I C, Jones P D, Shiyatov S G and Vaganov E A 2001 Low-frequency temperature variations from a northern tree ring density network *J. Geophys. Res.* **106** 2929–41

- [24] Stone D A, Allen M R, Stott P A, Pall P, Min S K, Nozawa T and Yukimoto S 2009 The detection and attribution of human influence on climate *Ann. Rev. Environ. Resour.* **34** 1–16
- [25] Harrison R G and Stephenson D B 2006 Empirical evidence for a nonlinear effect of galactic cosmic rays on clouds *Proc. R. Soc. A* **462** 1221–33
- [26] Haigh J D 1996 The impact of solar variability on climate *Science* **272** 981–4
- [27] Gray L J, Crooks S, Pascoe C, Sparrow S and Palmer M 2004 Solar and QBO influences on the timing of stratospheric sudden warmings *J. Atmos. Sci.* **61** 2777–96
- [28] Simpson I R, Blackburn M and Haigh J D 2009 The role of eddies in driving the tropospheric response to stratospheric heating perturbations *J. Atmos. Sci.* **66** 1347–65
- [29] Slonosky V C, Jones P D and Davies T D 2001 Instrumental pressure observations and atmospheric circulation from the 17th and 18th centuries: London and Paris *Int. J. Climatol.* **21** 285–98
- [30] Luterbacher J *et al* 2001 The late Maunder minimum (1675–1715)—a key period for studying decadal scale climatic change in Europe *Clim. Change* **49** 441–462
- [31] Xoplaki E, Luterbacher J, Paeth H, Dietrich D, Steiner N, Grosjean M and Wanner H 2005 European spring and autumn temperature variability and change of extremes over the last half millennium *Geophys. Res. Lett.* **32** L15713
- [32] Wanner H, Pfister C, Brázdil R, Frich P, Frydendahl K, Jónsson T, Kington J, Lamb H H, Rosenørn S and Wishman E 1995 Wintertime European circulation patterns during the late Maunder Minimum cooling period (1675–1704) *Theor. Appl. Climatol.* **51** 167–75
- [33] Barriopedro D, García-Herrera R, Lupo A R and Hernández E 2006 A climatology of Northern Hemisphere blocking *J. Clim.* **19** 1042–63
- [34] Yiou P and Masson-Delmotte V 2005 Trends in sub-annual climate variability since the Little Ice Age in western Europe *C. R. Geosci.* **337** 1001–12
- [35] Woollings T, Charlton-Perez A, Ineson S, Marshall A G and Masato G 2010 Associations between stratospheric variability and tropospheric blocking *J. Geophys. Res.* **115** D06108
- [36] Huth R, Pokorná L, Bochníček J and Hejda P 2006 Solar cycle effects on modes of low-frequency circulation variability *J. Geophys. Res.* **111** D22107
- [37] Huth R, Kyselý J, Bochníček J and Hejda P 2008 Solar activity affects the occurrence of synoptic types over Europe *Ann. Geophys.* **26** 1999–2004
- [38] Bochníček J and Hejda P 2005 The winter NAO pattern changes in association with solar and geomagnetic activity *J. Atmos. Sol.-Terr. Phys.* **67** 17–32
- [39] Solanki S K, Usoskin I G, Kromer B, Schüssler M and Beer J 2004 Unusual activity of the Sun during recent decades compared to the previous 11,000 years *Nature* **431** 1084–7
- [40] Abreu J A *et al* 2008 For how long will the current grand maximum of solar activity persist? *Geophys. Res. Lett.* **35** L20109
- [41] Lean J L and Rind D H 2008 How natural and anthropogenic influences alter global and regional surface temperatures: 1889 to 2006 *Geophys. Res. Lett.* **35** L18701